

Multiscale nature of hysteretic phenomena: Application to CoPt-type magnets

K. D. Belashchenko and V. P. Antropov
Ames Laboratory, Ames, Iowa 50011

We suggest a workable approach for the description of multiscale magnetization reversal phenomena in nanoscale magnets and apply it to CoPt-type alloys. We show that their hysteretic properties are governed by two effects originating at different length scales: a peculiar splitting of domain walls and their strong pinning at antiphase boundaries. We emphasize that such multiscale nature of hysteretic phenomena is a generic feature of nanoscale magnetic materials.

The problem of magnetization reversal (MR) is a central and longstanding problem in the theory of magnetism. Main complications in its treatment stem from the fact that effects due to magnetostatic and elastic forces manifest themselves in the whole nanoscale range while local interactions must still be treated on the atomistic scale. As the length scale increases, new physical effects arise, but coarse-graining over the lower-scale degrees of freedom is not easily accomplished. Specifically, MR is realized by motion of domain walls (DW), the two-dimensional surfaces where magnetization changes its direction. DW's may easily move unless they are pinned by defects, which implies that MR properties are not intrinsic and depend strongly on the microstructure. Experimentally, this results in huge variations of the coercive force H_c and other properties depending on material processing. It is crucial to address the DW structure and its interaction with microstructure on different length scales ranging from interatomic to submicron.

In modern micromagnetic methods [1] complex microstructures of hard magnets are defined by (usually piecewise constant) fields of macroscopic material properties such as the exchange constant $A(\mathbf{r})$ and the magnetocrystalline anisotropy (MCA) constant $K(\mathbf{r})$. Such calculations were mainly focussed on the role of grain boundaries; since they are extremely hard to describe microscopically, their properties are postulated in an *ad hoc* manner making reliable predictions problematic. From the other hand, typical microstructures of hard magnets with $L1_0$ crystal structure including CoPt, FePt and FePd are dominated by other defects [2, 3, 4, 5, 6, 7], antiphase boundaries (APB) and twin boundaries (TB), which are crystallographically coherent and easier to treat than grain boundaries. Although these materials were used and studied for many decades and the formation of their microstructure is well understood, the mechanism of MR is still a mystery. The goal of the present letter is to lay the foundation of a consistent multiscale theory of MR in CoPt type magnets.

Microstructural evolution during $L1_0$ ordering is strongly affected by tetragonal lattice distortions [5, 6]. After a relatively short 'tweed' stage of annealing after quench, when the ordered domains achieve some characteristic size $l_0 \sim 10$ nm, they develop so-called polytwinning, i.e. the formation of regular arrays ('stacks')

of ordered bands (' c -domains') separated by TB's [2, 3, 4, 5, 6]. The tetragonal axes c of the c -domains (pointing along one of the three cubic axes of the parent fcc phase) alternate regularly making 90° angles between the adjacent domains (below we use the obvious terms 'X-domain', 'XY-stack', etc.). In addition to polytwinning, the observed and simulated microstructures always contain a high density of APB's in the c -domains [3, 4, 5, 6, 7].

Polytwinned magnets were extensively studied with analytical micromagnetic methods [2]. Due to high MCA the DW width $\delta = \pi\sqrt{A/K}$ is quite small (5–10 nm), while the anisotropy field $H_a = 2K/M$ (M is the saturation magnetization) significantly exceeds the typical magnetostatic field $H_m = 4\pi M$ (parameter $\eta = H_m/H_a$ is close to 0.1 in CoPt and FePt and 0.38 in FePd [2]). Therefore, at $d \gtrsim \delta$ (d is the c -domain thickness) each c -domain may be regarded as an individual magnetic domain with intrinsic 90° DW's at the TB's [2]. It is assumed that MR is associated with 'macrodomain walls' (MDW) crossing many c -domains. Such MDW's were observed experimentally [2, 4], but their internal structure and mechanisms of coercivity are unknown [2].

Microscopic mean-field method. Consider a binary alloy AB with the classical Hamiltonian

$$H = H_{\text{conf}}\{n_i\} + \sum_{i<j} n_i n_j \left[-J_{ij} \vec{\mu}_i \vec{\mu}_j + \vec{\mu}_i \hat{D}_{ij} \vec{\mu}_j \right] + \sum_i n_i [\epsilon_i(\vec{\mu}_i) - \mathbf{H}_0 \vec{\mu}_i] \quad (1)$$

where H_{conf} is the configurational part of the Hamiltonian; i and j run over lattice sites; $n_i = 1$ if site i is occupied by a magnetic atom A and $n_i = 0$ otherwise (let B be non-magnetic for simplicity); $\vec{\mu}_i$ is the rigid classical magnetic moment of the atom at site i ; J_{ij} , the Heisenberg exchange parameters; \mathbf{H}_0 , the external magnetic field; $\epsilon_i(\vec{\mu}_i)$, the MCA energy equal to $-b_i(\vec{\mu}_i \mathbf{e}_i)^2$ for easy-axis anisotropy; and \hat{D}_{ij} , the magnetic dipole-dipole interaction tensor.

The free energy in the mean-field approximation (MFA) may be related to the 'mean fields' $\mathbf{H}_i = \mathbf{H}_0 + \sum_j (J_{ij} - \hat{D}_{ij}) c_j \mathbf{m}_j$ where $\mathbf{m}_i = \langle \vec{\mu}_i \rangle$ and $c_i = \langle n_i \rangle$ are

local magnetizations and concentrations, respectively:

$$F = -E_{J,DD} - T \sum_i c_i \ln \int d\hat{\mu}_i \exp[\beta(\mathbf{H}_i \hat{\mu}_i - \epsilon_i)]. \quad (2)$$

Here $E_{J,DD} = \sum c_i c_j \mathbf{m}_i (-J_{ij} + \hat{D}_{ij}) \mathbf{m}_j$ is the total exchange and dipole-dipole energy. Equilibrium states may be found using self-consistency relation $\mathbf{m}_i = -\partial F / \partial \mathbf{H}_i$.

If magnetization $\mathbf{M}(\mathbf{r})$ slowly varies in space and is constant in magnitude, Eq. (2) reduces to the micromagnetic free energy [9]. In this case all choices of J_{ij} and b_i in the defect-free regions are equivalent if they produce the same macroscopic properties A and K . However, variation of J_{ij} and b_i near defects like APB's must be studied using first-principles techniques. Microscopic MFA calculations with these parameters may be used to describe DW interaction with a defect at the length scale of δ . At larger, microstructural length scales micromagnetic methods [1] may be used with singularities of A and K at the defects. However, in hard magnets the microscopic approach also turns out to be convenient for the studies of regions containing up to $\sim 10^6$ atoms; in such calculations some model J_{ij} and b_i reproducing the actual defect properties may be used.

Below, we first address the equilibrium structure of MDW's in a defect-free system and find a peculiar MDW splitting phenomenon. Then we explore the behavior of MDW's in external field, briefly report our results for pinning at APB's, and finally deduce the combined effect of MDW splitting and pinning on coercivity.

Equilibrium macrodomain walls. It is convenient to use the body-centered tetragonal (bct) representation of the fcc lattice (with $c/a = \sqrt{2}$ and c equal to the fcc lattice parameter). Two opposite edges of a rectangular simulation box are aligned with the (110) TB's in the XY-stack; MDW's are normal to them. The boundary conditions are periodic, and the dipole-dipole fields are computed using the Fourier transforms.

Equilibrium MDW's of two characteristic $(1\bar{1}0)$ and (001) orientations are shown in Fig. 1 for the CoPt model. Infinite stack of c -domains is assumed with ideal TB's in the (110) planes. Fully ordered c -domains have the same thickness $d = 64a \simeq 17$ nm, which corresponds to an early stage of annealing shortly after the polytwinned stacks are formed [4, 6]. The anisotropy is uniaxial with \mathbf{e}_i pointing along the local direction of the tetragonal axis and $b_i = b$. Room temperature $T = 0.4T_c$ is assumed everywhere (for CoPt $T_c \simeq 720$ K). For simplicity, only $3d$ -metal atoms are assumed to have magnetic moment μ . Parameters b and μ were chosen so that MFA gives experimental room-temperature values of $K = 4.9 \times 10^7$ erg/cm³ and $\eta = 0.082$ for CoPt [2]. The parameters J_{ij} for nearest and next-nearest neighbors were chosen as $J_2/J_1 = 2/3$, $J_3/J_1 = 1/6$; A is isotropic with this choice.

MDW's of both orientations shown in Fig. 1 have a

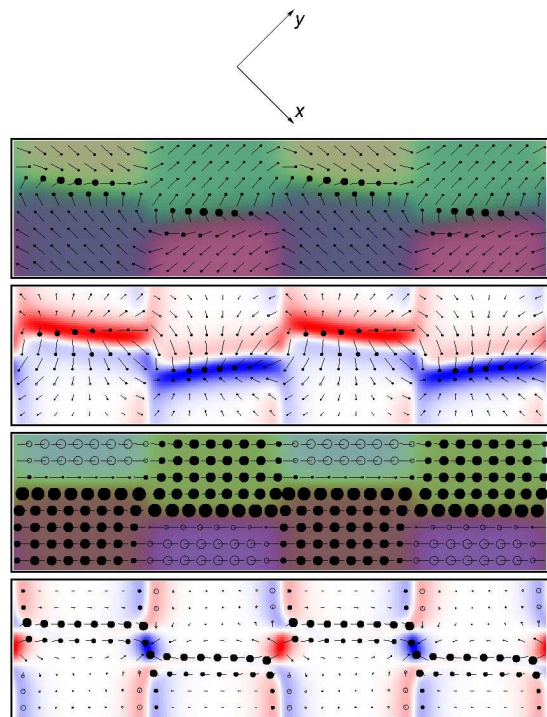


FIG. 1: Macrodomain walls in an ideal XY-stack with $d = 64a_{\text{bct}}$ oriented normal to: (a),(b) $(1\bar{1}0)$; (c),(d) (001) . Frames (a),(c): magnetization $\mathbf{M}(\mathbf{r})$ (arrows and color); (b),(d): dipole fields (arrows) and magnetic charge density $\rho = -\text{div } \mathbf{M}$ (color). The axes at top refer to (a),(b); in (c),(d) they are rotated 90° around the horizontal line. Sticks with circles show vector directions for cells $i = (8n_1 + 4, 8n_2 + 4, 1)$ with integer n_1, n_2 . The length of a stick (up to the center of the circle) is proportional to the vector projection onto the graph plane; the diameter of full (open) circles, to the positive (negative) out-of-plane component. Small points at the end of long sticks show their direction. Color in (a),(c) (guide to the eye) is obtained by mixing red, green and blue according to the values of three vector components. In (b),(d) the intensity of red (blue) color is proportional to the relative density of positive (negative) magnetic charges $\rho/|\rho_{\text{max}}|$. Twin boundaries are vertical. The simulation boxes had $512 \times 128 \times 1$ and $512 \times 128 \times 2$ bct cells for $(1\bar{1}0)$ and (001) MDW's, respectively. Figures are 2 times higher than the simulation boxes; they are trimmed at top and bottom to conserve space.

peculiar feature which turns out to be the key to the understanding of MR in polytwinned magnets: the DW segments (DWS) located in adjacent c -domains are displaced in respect to each other. Such configuration with regularly alternating displacements is beneficial for the exchange energy because magnetization within each DWS is parallel to that in the adjacent c -domains (note that the color of horizontal DWS's in Fig. 1a,c matches that of adjacent c -domains). The magnetostatic energy for this MDW configuration is higher compared to the rectilinear one due to the presence of short magnetically charged (in micromagnetic terms [9]) segments of 90° DW's at the TB's (note the red and blue 'blobs' in

Fig. 1d). Actual MDW configuration emerges as a result of competition between these interactions. However, due to small η the dipole-dipole interaction is, in fact, unimportant at the length scale of δ .

As it is clear from Fig. 1, the magnetic charges both at the DWS's of a $(1\bar{1}0)$ MDW and at the TB's alternate in sign, so that each MDW is magnetically uncharged as a whole, and its magnetic field quickly falls off at $r \gtrsim d$. DWS's of (001) MDW's do not carry magnetic charge.

The orientation of DWS's within c -domains in $(1\bar{1}0)$ MDW is determined by the anisotropy of the exchange constant $\alpha_A = A_{\perp}/A_{\parallel}$ (A_{\perp} and A_{\parallel} are values of A normal and parallel to c), and by the parameter $\xi = \eta d/\delta$. At $\xi \ll 1$ the DW orientation is determined solely by α_A . At $\xi \gg 1$ the DW aligns parallel to the tetragonal axis, and α_A is irrelevant. The $(1\bar{1}0)$ MDW shown in Fig. 1a,b is in the crossover region with $\xi \sim 0.2$ and $\alpha_A = 1$.

Partial macrodomain walls. MDW's behave remarkably in external magnetic field \mathbf{H}_0 because DWS's are held together only by magnetostatic forces. If these forces were absent ($\eta \rightarrow 0$ limit), each DWS would be able to move freely until it meets another DWS in an adjacent c -domain. Some of this freedom remains at small η . Consider an XY-stack with (110) TB's, as above. Component H_z does not exert any force on DWS's, and the effect of \mathbf{H}_0 on MDW's depends only on the orientation of its projection \mathbf{H}_{\perp} on the xOy plane. If \mathbf{H}_{\perp} is normal to the TB's ($H_x = H_y$), then the forces acting on all DWS's are in the same direction, and both MDW's shown in Fig. 1 move as a whole like usual DW's in a homogeneous crystal. However, if \mathbf{H}_{\perp} is parallel to the TB's ($H_x = -H_y$), the forces acting on X- and Y-DWS's differ in sign, and the total force acting on the MDW is zero.

Let us call a set of DWS's of a MDW in all even or odd c -domains as a *partial macrodomain wall* (PMDW), e.g. X-PMDW. There are two MDW realizations differing in the sign of the relative displacement L of the two PMDW's. For one of them \mathbf{H}_{\perp} increases $|L|$ ('splitting'), and for the other, reduces it ('swapping'). If \mathbf{H}_{\perp} is inverted, splitting turns to swapping and vice-versa. Accordingly, two threshold fields may be introduced. Let us fix, for instance, Y-PMDW and examine the effect of H_x on X-PMDW. The *threshold splitting field* H_{sp} is the minimal value of H_x required to move the X-PMDW far from the Y-PMDW. The *threshold swapping field* H_{sw} is required to 'drag' the X-PMDW through Y-PMDW in the opposite direction, overcoming the exchange barriers at the TB's. H_{sw} is of lesser importance than H_{sp} because even if $H_{sp} < H_{sw}$, the existence of some MDW's in the 'splitting relation' with \mathbf{H}_x is sufficient to complete the MR. Note also that $H_{sw} \propto d^{-1}$ and quickly falls off with increasing d . Both H_{sp} and H_{sw} are 'intrinsic' properties for a given d , i.e. they exist even if there are no defects (APB's) in the c -domains.

H_{sp} may be easily estimated micromagnetically for a (001) MDW. When its two PMDW's are displaced at dis-

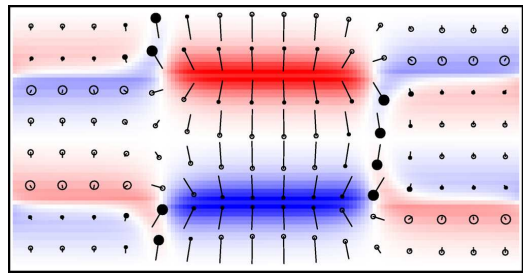


FIG. 2: Split (001) macrodomain wall in a stack with $d = 32a_{\text{bct}}$. Presentation is similar to Fig. 1d.

tance L , the alternating magnetic charges appearing at the TB's form a regular stack of 'capacitors' (see Fig. 2). For $L \gtrsim d$, the magnetic field is concentrated inside these capacitors, and the total magnetostatic energy is proportional to L ; the coefficient in this proportionality determines H_{sp} . Such calculation gives $H_{sp} = \pi M$ (or, alternatively, $H_{sp} = H_a \eta/4$). The splitting threshold for $(1\bar{1}0)$ MDW is larger because of the magnetic charges on its segments. In the above estimate we neglected the deviation of \mathbf{M} from the easy axis at distances $\sim \delta$ from the TB's, which reduces H_{sp} for small d .

Thus, at $\eta \ll 1$ we have $H_{sp} \ll H_a$. In particular, using the room-temperature values of M [2], we obtain H_{sp} of 2.5 kOe for CoPt and 3.5 kOe for FePt and FePd. These values are close to the typical fields at which hysteresis is observed in these magnets. Quite naturally, they are much less than the coercive fields corresponding to uniform rotation of magnetization in the c -domains [2]. A peculiar feature of a PMDW in the polytwinned crystal is that it separates qualitatively different magnetic domains with different free energies, and hence there is an intrinsic force acting on an isolated PMDW (its density per unit cross-section of the c -domain is $f_s = 2MH_{sp}$).

Domain wall segments, pinning and coercivity. Real polytwinned alloys, as we noted above, usually contain a high density of APB's in the c -domains. It is known that DW's may be pinned by APB's [10], and it was argued that this mechanism may explain high coercivity of CoPt type alloys [7, 8]. Here we show that this pinning is indeed quite strong, but the MDW 'dissociation' into segments also has a profound effect on MR.

The APB pattern within c -domains determines the statistical properties of the random value $U(x)$ where x is the coordinate of a DWS, and U is its APB-induced excess free energy. For the following basic consideration we assume that $U(x)$ describes a distribution of similar pinning centers with the typical distance l_d between them. The maximal slope of $U(x)$ determines the *unpinning threshold* H_u , i.e. the value of the field $\mathbf{H}_0 \parallel c$ required to unpin a single c -DWS. Thus, in the absence of magnetostatic forces at $H_0 < H_u$ each c -DWS is pinned, and at $H_0 > H_u$ it can move freely to the surface of the polytwinned stack. These assumptions are obvious

for patterns with isolated APB's as in Fig. 5 of Ref. [3] where $l_d \sim 5-10d$; however, main features of more complex patterns [4, 5, 6, 8] may also be described by some characteristic values of H_u and $l_d \lesssim d$.

The maximum possible H_u is achieved when DWS's are parallel to isolated plain APB's. To evaluate this maximum in the studied alloys, we explored the modification of exchange and anisotropy at an isolated (101)-oriented APB in CoPt, FePt and FePd using the tight-binding linear muffin-tin orbital method. We found that MCA is strongly suppressed at the APB leading to a DW *attraction* to the APB with H_u of about 11, 7 and 1.5 kOe for CoPt, FePt and FePd, respectively. These values significantly exceed the observed coercivities [8]. Since high MCA is associated with L1₀ ordering, it is natural that local disorder at an APB suppresses MCA.

Let us now explore the role of intrinsic magnetostatic forces in MR. We restrict ourselves to the case of $\mathbf{H}_0 \parallel Ox$ in a single crystal with different types of polytwinned stacks ('single crystal' refers to the parent fcc lattice). Such field does not affect YZ-stacks, except for a reversible transverse magnetization. In other stacks \mathbf{H}_0 exerts a force density $f = 2MH_0$ on X-DWS's *only*.

From our definition of H_{sp} it follows that if *c*-PMDW in X*c*-stack (*c* = Y or Z) is held in place (e.g., by pinning), then the free (unpinned) X-PMDW moves to infinity at $H_x \geq H_{sp}$ (neglecting the demagnetizing effects). At $H_x < H_{sp}$ the X-PMDW moves to a finite distance $L(H_x)$ from the *c*-PMDW. By definition, $L(H_{sp}) = \infty$. Except for a close vicinity of H_{sp} , $L \lesssim d$.

The path of MR differs qualitatively in two cases: (a) $H_{sp} > H_u$, and (b) $H_{sp} < H_u$. In case (a) the MDW can only move as a whole (intrinsic forces f_s are strong enough to unpin a PMDW), but DWS's may to some extent 'adapt' to the local pinning potential. Let us define the characteristic displacement l_m 'allowed' by magnetostatic forces as $l_m = L(H_u)$. Obviously, l_m increases with H_u , and $l_m \rightarrow \infty$ at $H_u \rightarrow H_{sp}$. If $l_m > l_d$, the effective unpinning field of the MDW is $H_U \sim 2H_u$ (\mathbf{H}_0 affects one half of the DWS's, while all DWS's can be effectively pinned). However, as l_m becomes smaller than l_d , H_U is quickly reduced, because only a fraction of DWS's can be pinned simultaneously (MDW is effectively 'rigid' and can not make 'kinks' comparable with l_d).

Now, in case (b) the MDW may split in two PMDW's at sufficiently large \mathbf{H}_0 . The MDW is 'soft', and each DWS can be effectively pinned. During the whole cycle of remagnetization pinned Y- and Z-PMDW's do not move at all, and hence the intrinsic (magnetostatic) force acting on a moving X-PMDW will change its sign every time that it crosses, e.g., an Y-PMDW (in XY-stack). Thus, for an X-PMDW we have $H_U = H_u + H_{sp}$. Different MR properties may, in principle, be observed if the sample was previously magnetized to saturation by \mathbf{H}_0 along, e.g., (111). In this case there are no Y- and Z-PMDW's, and in some stacks the switching threshold

is $H_U = H_u - H_{sp}$. The hysteresis loop in this case may have a peculiar double-step feature with magnetization jumps at $H_0 = H_u \pm H_{sp}$. Such 'hysteresis memory' effects provide a test of the $H_{sp} < H_u$ relation and may be used to design 'programmable' magnets.

Thus, for an initially demagnetized sample with the given H_u the coercive force H_c first rises with H_{sp} , reaches its maximum $\sim 2H_u$ at $H_{sp} \approx H_u$, stays roughly constant in the range $\infty > l_m > l_d$, and finally falls off at $l_m < l_d$. High coercivity of CoPt is probably due to the fact that this magnet with suitable processing is close to the optimal $H_{sp} \sim H_u$ condition. By contrast, in FePd H_{sp} is too large ($H_{sp}/H_u \approx 2.3$ even for maximal possible H_u), so that $l_m \ll d$; this conclusion agrees with the relatively small observed H_c/H_a ratio.

In our analysis we neglected the demagnetizing fields. Close to saturation they are comparable to H_{sp} , but they have little effect on H_c , because they are small when the total magnetization is close to zero.

In conclusion, we developed a workable technique for the description of multiscale MR phenomena in hard magnets and applied it to CoPt-type alloys. We have shown that coercivity of these materials has at least two sources originating at different length scales: strong pinning of MDW's by APB's and their splitting at TB's. This DW splitting seems to be a generic effect that may also affect MR in other groups of materials, including some nanostripes [11] and multilayers; it may also occur at grain boundaries of certain misorientations.

The authors are grateful to V.G. Vaks for useful discussions. This work was carried out at Ames Laboratory, which is operated for the U.S. Department of Energy by Iowa State University under Contract No. W-7405-82. This work was supported by the Director for Energy Research, Office of Basic Energy Sciences of the U.S. Department of Energy.

-
- [1] R. Fischer and H. Kronmüller, Phys. Rev. B **54**, 7284 (1996); J. Fidler, T. Schrefl, J. Phys. D **33**, R135 (2000).
 - [2] N.I. Vlasova, G.S. Kandaurova and N.N. Shchegoleva, J. Magn. Magn. Mater. **222**, 138 (2000).
 - [3] C. Leroux, A. Loiseau, D. Broddin and G. van Tendeloo, Phil. Mag. B **64**, 58 (1991).
 - [4] C. Yanar, J.M.K. Wiezorek and W.A. Soffa, in *Phase Transformations and Evolution in Materials*, ed. P. Turchi and A. Gonis (TMS, Warrendale, 2000), p. 39.
 - [5] L.-Q. Chen, Y. Wang and A.G. Khachatryan, Phil. Mag. Lett. **65**, 15 (1992).
 - [6] K.D. Belashchenko, I.R. Pankratov, G.D. Samolyuk and V.G. Vaks, J. Phys.: Condens. Matter **14**, 565 (2002).
 - [7] Ya.S. Shur *et al.*, Phys. Met. Metallogr. **26**, 241 (1968).
 - [8] B. Zhang and W.A. Soffa, Phys. Stat. Sol. (a) **131**, 707 (1992); Scr. Met. Mater. **30**, 683 (1994).
 - [9] A. Aharoni, *Introduction to the theory of ferromagnetism* (Clarendon, Oxford, 1996).

- [10] H. Kronmüller, *J. Magn. Magn. Mater* **7**, 341 (1978).
- [11] M. Pratzner *et al.*, *Phys. Rev. Lett.* **87**, 127201 (2001).